*Article*

# Genomic Analysis of Two Representative Strains of *Shewanella putrefaciens* Isolated from Bigeye Tuna: Biofilm and Spoilage-Associated Behavior

Zhengkai Yi [1,2,3] and Jing Xie [1,2,3,4,*]

1 College of Food Science & Technology, Shanghai Ocean University, Shanghai 201306, China; d200300064@st.shou.edu.cn
2 Shanghai Professional Technology Service Platform on Cold Chain Equipment Performance and Energy Saving Evaluation, Shanghai 201306, China
3 National Experimental Teaching Demonstration Center for Food Science and Engineering, Shanghai 201306, China
4 Shanghai Engineering Research Center of Aquatic Product Processing & Preservation, Shanghai 201306, China
* Correspondence: jxie@shou.edu.cn; Tel.: +86-02161900391

**Abstract:** *Shewanella putrefaciens* can cause the spoilage of seafood and shorten its shelf life. In this study, both strains of *S. putrefaciens* (YZ08 and YZ-J) isolated from spoiled bigeye tuna were subjected to in-depth phenotypic and genotypic characterization to better understand their roles in seafood spoilage. The complete genome sequences of strains YZ08 and YZ-J were reported. Unique genes of the two *S. putrefaciens* strains were identified by pan-genomic analysis. In vitro experiments revealed that YZ08 and YZ-J could adapt to various environmental stresses, including cold-shock temperature, pH, NaCl, and nutrient stresses. YZ08 was better at adapting to NaCl stress, and its genome possessed more NaCl stress-related genes compared with the YZ-J strain. YZ-J was a higher biofilm and exopolysaccharide producer than YZ08 at 4 and 30 °C, while YZ08 showed greater motility and enhanced capacity for biogenic amine metabolism, trimethylamine metabolism, and sulfur metabolism compared with YZ-J at both temperatures. That YZ08 produced low biofilm and exopolysaccharide contents and displayed high motility may be associated with the presence of more a greater number of genes encoding chemotaxis-related proteins (*cheX*) and low expression of the *bpf* A operon. This study provided novel molecular targets for the development of new antiseptic antisepsis strategies.

**Keywords:** *Shewanella putrefaciens*; complete genome sequence; spoilage; biofilm; extracellular protease

## 1. Introduction

Aquatic products are regarded as an important food source globally owing to its low-fat content and rich animal protein. However, aquatic products are highly perishable foods after death, even under refrigerated conditions. Microorganisms are essential in the spoilage of aquatic products, even with the rapid development of modern preservation technologies [1,2]. The main microorganisms responsible for food spoilage are known as specific spoilage organisms (SSOs) [3]. These SSOs can break down nitrogenous compounds (amino acids and proteins) in aquatic products into ammonia, biogenic amines, sulfides, and volatile compounds (including aldehydes, ketones, alcohols, and organic acids), leading to the degradation of sensory properties and making fish products unacceptable [4,5].

Although low temperatures inhibit the growth and metabolism of most microbes, many studies showed that *S. putrefaciens* can reduce the shelf life of refrigerated seafood, such as tuna [6], Pacific white shrimp [7], and cod [8]. Most *S. putrefaciens* strains can reduce trimethylamine oxide (TMAO) to trimethylamine (TMA) [9] and decarboxylate specific amino acids to biogenic amines, including putrescine, histamine, and cadaverine [10].

*S. putrefaciens* can also form biofilms in the aquatic matrix to enhance its adsorption capacity [11], degrade myofibrillar proteins in fish meat, and oxidize lipids [12]. However, relatively few studies have focused on the genome of *S. putrefaciens*, when investigating its relationship with its spoilage potential.

In recent years, genome-wide mining has contributed to the understanding of spoilage-associated metabolic pathways in SSO [13]. Exploring spoilage-related metabolic pathways by gene mining is essential for gaining insight into the spoilage behavior of spoilage bacteria. Chen et al. [14] reported the genome-wide sequence of *S. putrefaciens* WS13. However, the spoilage potential of *S. putrefaciens* has not been resolved at the genomic level. In addition, *S. putrefaciens* possesses good cold adaptability under low temperature conditions, which may be related to the expression of genes regulating fatty acid metabolism [15]. To date, there are no studies reporting the association between spoilage-related genes and phenotypic traits of *S. putrefaciens*.

The aim of this work was to reveal the mechanisms of *S. putrefaciens* underlying the spoilage activity at the genetic level. To achieve this, the whole genome sequences of two *S. putrefaciens* strains with different spoilage abilities were studied and compared to reveal the spoilage-associated genetic differences and identify key spoilage-causing genes. Phenotypes and related genotypes, including growth under stress, biofilm formation, motility, protein hydrolysis, lipolytic activity, TMA, and hydrogen sulfide ($H_2S$) production capacity, were investigated in both strains to elucidate the relationship between spoilage-related genes and bacterial phenotypes. This study is helpful for the search for new spoilage factors of *S putrefaciens* and can be further verified by molecular biology methods. Our results provide new directions in the advancement of spoilage detection and prevention methods and identify novel involved in microbe-mediated fish spoilage.

## 2. Materials and Methods

### 2.1. S. putrefaciens Strains and Cultures

*S. putrefaciens* YZ08 and YZ-J strains were isolated from spoiled bigeye tuna during 4 °C storage for 8 days. Spoiled bigeye tuna was determined by sensory evaluation as described by Yi and Xie [16]. A total of 25 g of spoiled tuna flesh was homogenized in 225 mL of 0.85% sterile saline and serial dilutions were prepared. For bacterial purification, all the isolates from the highest dilution plate (nutrient broth, containing 30–100 isolates) were incubated in nutrient broth for 48 h at 30 °C and were subsequently purified on iron agar (IA) at 30 °C. *Shewanella* spp. is an $H_2S$-producing bacterium that produces black clones on IA. The $H_2S$-producing bacteria strains were dominant species (20/50). All purified colonies were identified by 16S rRNA gene sequencing using primers 27F (5′-AGAGTTTGATCMTGGCTCAG-3′) and 1492R (5′-GGTTACCTTGTTACGACTT-3′). In a preliminary experiment, 14 *S. putrefaciens* strains were inoculated into sterilized tuna meat. The sterile fish blocks were prepared according to Li et al. [12]. After inoculation, fish blocks were placed in sterile bags for refrigeration at 4 °C for 8 days. Through preliminary sensory identification, the clones associated with the best and the worst quality of inoculated fish meat were selected for further study (identified as *S. putrefaciens* YZ08 and YZ-J). Purified strains were stored in tryptose soya broth (TSB) contained 25% glycerine at −80 °C. Before use, stains were pre-cultured in TSB for 18 h and then cultured in TSB at 30 °C for 8 h. Bacterial cell cultures at the logarithmic phase (8 log CFU/mL, $OD_{600} \approx 0.8$) were used for inoculation in subsequent experiments (including bacterial DNA extraction, growth, biofilm formation, motility assays, protein hydrolysis, lipolysis, measurement of spoilage-related indicators and RT-qPCR).

### 2.2. Complete Genome Sequencing of S. putrefaciens YZ08 and YZ-J and Functional Annotation

The high-quality genomic DNA was extracted from two *S. putrefaciens* strains with a Bacterial DNA Kit (OMEGA). Genome sequencing was performed by Shanghai Biozeron Technology Co. Ltd. (Shanghai, China) using Illumina NovaSeq 6000 sequencing platform and PacBio RSII platform. A total of 3μg of genomic DNA (150 ng/μL) were used for

sequencing library construction. Two libraries with insert sizes of approximately 400 bp and 15–20 kb was constructed and sequenced on an Illumina NovaSeq 6000 sequencing platform and a PacBio RSII platform, respectively. Raw data obtained from the Illumina NovaSeq 6000 sequencing platform and PacBio RSII platform were quality controlled (remove low-quality reads and repeat reads) for further assembly. First, Illumina sequencing data were assembled using SOAPdenova v1.05 and then were compared with the PacBio sequencing data corrected errors. Next, the corrected data were assembled using Celera Assembler v8.0 to generate the scaffolds. Finally, the assembled scaffolds were mapped back to Illumina clean reads using GapCloser v1.12 for gap closing.

For the identification of genes associated with spoilage behavior, key proteins related to spoilage metabolism were collected. Candidate genes were obtained by searching all predicted proteins in the YZ08 and YZ-J genomes (E-value = 1E10; coverage $\geq$ 70%; identity $\geq$ 35%) using the blastP algorithm. Candidate genes were further confirmed by protein, COG, and GO functional annotation [18]. In addition, relevant metabolic genes were obtained directly by KEGG pathway analysis.

Functional annotation was performed using databases of non-redundant (NR) protein, Kyoto Encyclopedia of Genes and Genomes (KEGG), Swiss-Prot, Cluster of Orthologous Groups (COG), and Gene Ontology (GO). Genomic tRNAs and rRNAs were analyzed using tRNAscan-SE v1.3.1 (University of California, California, USA) and RNAmmer v1.2 (Technical University of Denmark, Lyngby, Denmark). Secretory proteins were predicted using the signal peptide prediction tool signalP v5.0 (Technical University of Denmark, Lyngby, Denmark) [17].

*2.3. Pan-Genome Analysis and Genome Mining of S. putrefaciens YZ08 and YZ-J*

Pairwise genome alignment and visualization analysis of *S. ptrefaciens* YZ08 and YZ-J strains were performed using MAUVE v2.4.0 (University of Wisconsin, Wisconsin, USA) [19]. All 10 *S. putrefaciens* complete genomes in NCBI were subjected to pan/core genome analysis using the Bacterial Pan Genome Analysis tool (BPGA v1.3) [20]. The NCBI accession numbers for 8 of the 10 strains (excluding strains YZ08 and YZ-J) were NZ_CP066370, NZ_CP066369, NZ_CP046329, LR134303, CP015194, NZ_CP078038, NZ_CP028435, and CP070865. Each nucleotide sequence was analyzed using default settings. In BPGA, homologous protein clusters were identified using USEARCH (a clustering tool) with a threshold of 0.5 and a phylogenetic tree was constructed based on the core genome. In addition, pan-genomic analysis was performed for strains YZ08 and YZ-J and unique genes were subjected to COG and KEGG functional annotation.

*2.4. Growth and Biofilm Formation of S. putrefaciens YZ08 and YZ-J under Stress Conditions*

*S. putrefaciens* strains YZ08 and YZ-J were pre-cultured in Luria Broth (LB) medium at 30 °C for 12 h. As a control, each strain was inoculated into LB medium (pH 7.0) at a ratio of 1:1000 and incubated at 30 °C. To induce pH stress, the incubation temperature was kept constant (30 °C), but the pH of the LB medium was regulated to 6.0 using HCl; for NaCl stress, the NaCl concentration was adjusted to 5% by adding NaCl; for nutrient stress, the medium was diluted to 20% by adding distilled water; for temperature stress, the temperature was set at 4 °C. The bacteria were incubated under stress conditions for 168 h, and the total cell numbers was measured every 12 h. The total cell numbers were performed using plate count agar (PCA). Samples (1 mL) were serially diluted 10-fold with normal saline, and dilutions (0.1 mL) were spread on PCA. Plates were placed at 30 °C for 48 h and the total cell numbers were determined.

One milliliter of the dilutions (1:1000) of the above pre-cultures under various stress conditions were transferred to a 48-well plate. The plates were incubated under static conditions for 12, 24, 48, and 72 h. Biofilm formation were determinate by Yan and Xie [11]. Briefly, after culture, the supernatant was carefully discarded and the adherent cells were washed twice using saline (0.85%) and dried, then stained with 0.2% crystal violet for 15 min, washed and dried. Finally, it was dissolved in 95% ethanol to determine $OD_{600}$.

The total cell numbers in LB medium were also determined for normalization. The total cell numbers were determined by serial dilution as described in Section 2.4. The normalized results were expressed as the ratio of the $OD_{600}$ to the total number of cells.

### 2.5. Motility Assays

Swarming and swimming motility were measured on LB cultures containing 1.5% and 0.3% agar, respectively. Five microliters of bacterial culture ($1 \times 10^8$ CFU/mL) was dropped onto agar plates and incubated at 4 °C and 30 °C for 24, 48, and 72 h, and the diameters of the motility zones were measured, respectively.

### 2.6. Proteolytic and Lipolytic Activity

Proteolytic activity was measured on agar plates containing 5% skimmed milk (prepared with deionized water containing 5% skimmed milk powder and 2% agar), and lipolytic activity was measured on triglyceride agar (Solarbio, Beijing, China). Incubation was performed at 30 °C for 24, 48, and 72 h and 4 °C for 1, 2, and 4 days, respectively. Finally, proteolytic and lipolytic activity was determined according to the size of the produced halos.

### 2.7. Spoilage-Related Indicators

#### 2.7.1. Determination of TMA Content

Both strains of *S. putrefaciens* were inoculated in LB medium with TMAO (10 mM) and phosphate buffer saline (PBS, 100 mM) for 6 days at 4 °C and 48 h at 30 °C. TMA content was determined using the picric acid method [21].

#### 2.7.2. Determination of Biogenic Amines (BAs) Content

Both strains of *S. putrefaciens* were inoculated in LB medium with 0.5% L-ornithine monohydrochloride, L-arginine monohydrochloride, and lysine monohydrochloride with 0.005% pyridoxal-5′-phosphate for 6 days at 4 °C and 48 h at 30 °C. BAs were extracted according to Zhuang et al. [22], then separated and quantified using HPLC (SHIMADZU, LC-2010C HT, Kyoto, Japan) and COSMOSIL 5C18-PAQ columns after derivatization with dansyl chloride. Chromatographic conditions were according to Hong et al. [23].

#### 2.7.3. Preparation and Inoculation of Sterile Tuna Juice

Minced bigeye tuna back muscle (2 kg) was homogenized and boiled for 5 min with 2 L of distilled water. After adding 1.6 g/L TMAO, 40 mg/L L-cysteine and L-methionine, the filtrate was sterilized (121 °C, 15 min), yielding sterile bigeye tuna juice. The *S. putrefaciens* strains were separately inoculated into the fish juice at a final concentration of approximately 5 log CFU/mL and stored at 4 and 30 °C.

#### 2.7.4. Determination of $H_2S$ Content

The $H_2S$ content in fish juice was determined using a $H_2S$ concentration determination kit (Beijing Solabao, Beijing, China) and was expressed as μmol/mL.

#### 2.7.5. Determination of Exopolysaccharide Content and Extracellular Protease Activity

The exopolysaccharide of the inoculated fish juice was extracted according to the method of Feng et al. [24]. Nine milliliters of the inoculated fish juice was transferred to a six-well plate and incubated at 30 °C for 24, 48, and 72 h and at 4 °C for 1, 2, and 4 days, respectively. After carefully removing the cultures from the wells, the plate was cleaned 3 times with PBS to remove residual bacterial cells, 9 mL of PBS was added to each well, followed by sonication at 50 kHz for 5 min to dissolve the exopolysaccharides that had adhered to the walls of the wells (sonication can lyse cells in biofilms, resulting in the release of intracellular content). After centrifugation at $12,000\times g$ for 15 min at 4 °C, the obtained supernatant was used to measure exopolysaccharide content using the phenol-sulfuric acid

method [25], with glucose serving as a standard. Exopolysaccharide content was expressed as μg/mL.

Extracellular protease activity was determined according to Anbu [26], with some modifications. After centrifugation at $10,000\times g$ at 4 °C, the supernatant (500 μL) of the fish juice was added to an equal volume of 1% (*w/v*) casein substrate solution and incubated at 37 °C for 10 min. The reaction was terminated by adding 1 mL of TCA (20%). Finally, after centrifugation ($12,000\times g$, 10 min), the tyrosine content was determined using the Folin method [27]. The results were expressed as U/mL.

### 2.8. RT-qPCR

*S. putrefaciens* strains YZ08 and YZ-J were inoculated in LB medium at 30 °C until the log phase ($OD_{600}$ = 0.8). Total RNA was isolated from cultured cells using a Spin Column Bacteria Total RNA Purification Kit (Sangon, Shanghai, China) and reverse-transcribed into cDNA using an AMV First Strand cDNA Synthesis Kit (Sangon, Shanghai, China) with random primer p(dN)$_6$. qPCR was performed using SG Fast qPCR Master Mix (SYBR Green) (Sangon, Shanghai, China). The sequences of the primers used for qPCR are listed in Table S1. mRNA levels were normalized to that of the 16 S rRNA gene. The relative expression levels of each gene were determined using the $2^{-\Delta\Delta Ct}$ method [28].

### 2.9. Statistical Analysis

All data were analyzed using SPSS 19.0 (IBM, Chicago, IL, USA). The Student's *t*-test was employed for comparisons between two groups. One-way analysis of variance (ANOVA) with Duncan's post-hoc test was used for multiple groups. $p < 0.05$ were considered significant. All experiments were repeated at least three times.

## 3. Results and Discussion

### 3.1. Identification and Genome Properties of S. putrefaciens Strains YZ08 and YZ-J

The complete genome sequences were submitted in GenBank with accession numbers CP080633 (for YZ08) and CP080635 (for YZ-J). The genomes of *S. putrefaciens* YZ08 and YZ-J were determined to be 5,019,740 bp and 4,386,160 bp long, with average GC contents of 47.69% and 46.53%, respectively (Figure 1). Genes were annotated in multiple databases: NR, 4353 and 3806; Swiss-Prot, 3122 and 2842; COG, 3803 and 3464; KEGG, 2314 and 2194; GO, 1456 and 1429; VFDB, 527 and 535; and CAZy, 80 and 64. The genome contained 4443 and 3890 of genes in which 4301 and 3761 (96.80% and 96.68%) were assigned predicted proteins in YZ08 and YZ-J, respectively.
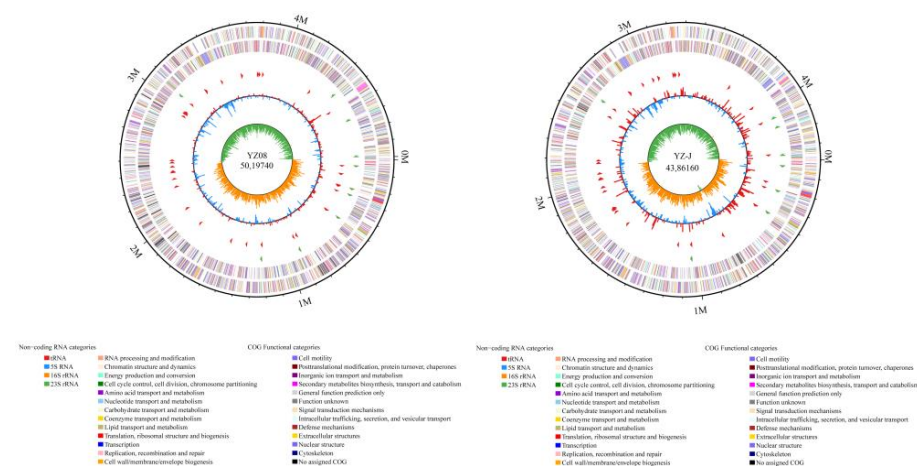


**Figure 1.** Map of the circular genome of *Shewanella putrefaciens* YZ08 and YZ-J. Genome size (first circle); coding DNA sequences on forward and reverse chains based on COGs categories (second and third circles); forward strand and reverse strand non-coding RNA (ncRNA) (fourth and fifth circle); guanine-cytosine (GC) content (sixth circle) and GC skew (fifth circle).

*3.2. Gene Function Analysis*

3.2.1. COG, GO, and KEGG Function Classification Analysis of the Two Strains

The unknown function category contained the largest number of genes for both *S. putrefaciens* strains. Both strains showed similar trends by which amino acid transport and metabolism, and energy production and conversion were the main COGs (Figure 2A). For energy production and conversion, the four most abundant COGs were COG0243, COG1012, COG0437, and COG1301 for YZ08, and COG1012, COG1053, COG0243, and COG0437 for YZ-J. COG0437 plays a crucial role in various electron transfer processes and several enzymatic reactions [29]. In response to environmental stresses, two Na+ ions were transported by COG1301 [30]. A similar COG functional classification was also found in *S. baltica* 128 (accession number CP028730). The differences in COG classification may be indicative of differences in metabolism and adaptability to the environment between the two strains. *S. putrefaciens* YZ08 and YZ-J genes were assigned to three function classifications by GO analysis (Figure 2B). The genes of the YZ08 and YZ-J strains in the biological process category were divided into 20 subfunctions, most of which were associated with cellular processes (GO:0009987), metabolic processes (GO:0008152), and response to stimulus (GO:0050896), which was consistent with the features reported for *Shewanella* spp. [13]. A similar GO functional classification was found for *S. putrefaciens* XY07 (accession number CP070865). The results for the KEGG pathway analysis of *S. putrefaciens* YZ08 and YZ-J genes are shown in Figure 2C,D. In the five KEGG pathways of the two strains, metabolism comprised the largest number of genes, followed by environmental information processing, cellular processes, and genetic information processing. Some pathways may be related to the distinct phenotypes shown by the two strains, such as two-component system (ko02020), microbial metabolism in diverse environments (ko01120), biosynthesis of amino acids (ko01230), bacterial chemotaxis (ko02030), ABC transporters (ko02010), biofilm formation-Vibrio cholerae (ko05111), flagellar assembly (ko02040), and cysteine and methionine metabolism (ko00270). Two-component systems (TCS) can translate extracellular signals into gene expression patterns that facilitate bacterial regulation of various physiological functions. ABC transporters (ko02010) are transmembrane proteins that use energy to transport substrates into the cell [31].

3.2.2. Genome Synteny and Pan-Genome Analysis

To explore the genetic differences between both strains, a genome synteny and pan-genome analysis were also investigated. As shown in Figure 3A, analysis of the genome sequences using MAUVE revealed that *S. putrefaciens* YZ08 and YZ-J shared many homologous regions. Although large genomic rearrangements and inversions were found in both strains, overall, the YZ08 and YZ-J genomes shared a large number of homologous regions.

The pan-genome of the 10 *S. putrefaciens* strains included 2637 core genes, 10,413 accessory genes and 1944 unique genes. Analysis of the pan-genome and core genome maps of oral *S. putrefaciens* (Figure 3B,C) showed that the number of the pan-genome increased, while that of the core genome decreased, indicating that *S. putrefaciens* has an open pan-genome and has the ability to survive in a variety of environments [13]. To investigate the phylogenetic relationships among the 10 strains, a phylogenetic tree was generated based on 2637 core genes (Figure 3D). *S. putrefaciens* YZ08 showed the greatest genetic relationship with the pap11 strain, while YZ-J was close to XY07, ATCC8071, and WS13.
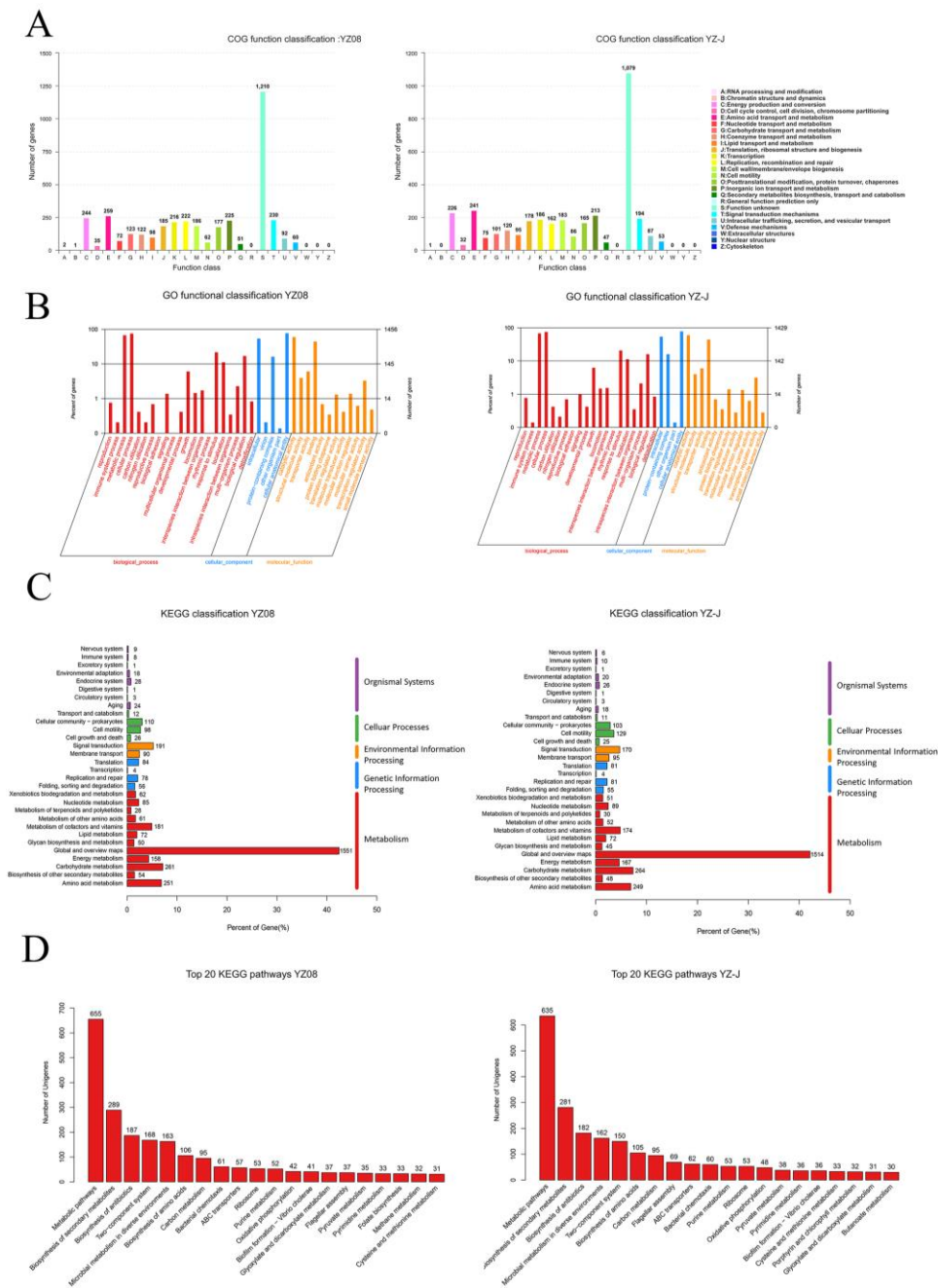
**Figure 2.** Whole genome sequence analysis of *S. putrefaciens* YZ08 and YZ-J. (**A**), Cluster of orthologous groups (COG). (**B**), Gene ontology (GO). (**C**), Kyoto Encyclopedia of Genes and Genomes (KEGG) Classification. (**D**), Top 20 KEGG pathways.

The pan-genome of *S. putrefaciens* YZ08 and YZ-J was investigated. The unique genes of both strains were listed in Tables S2 and S3. The unique genes of the two strains were annotated using KEGG and COG distribution (Figure 3E,F). In COG distribution, many unique genes of both strains were related to signal transduction mechanisms, which were involved in the regulation of various life activities of microorganisms. Key biofilm regulatory genes were identified in strain YZ08, annotated as COG5001 (diguanylate cyclase phosphodiesterase) in COG and classified as ko05111 (biofilm formation—Vibrio cholerae) in KEGG. These genes may play an inhibitory role in biofilm formation [32]. YZ08 may possess stronger amino acid metabolic activity than YZ-J owing to a greater abundance of COG0834 components (ABC-type amino acid transport/signal transduction system).

KEGG distribution showed that only YZ08 was involved in trimethylamine metabolism in methane metabolism (ko00680). Both strains contained genes coding for proteins with functions in membrane transport (ABC transporters). These transporters are involved in transporting a large number of endogenous substrates and exogenous compounds across lipid membranes and are associated with many important biological processes, such as the release of secreted proteins, cellular detoxification, lipid homeostasis, ion channel regulation, and ribosome assembly [33]. In addition, COG and KEGG distributions indicated that YZ08 possessed more cell motility-related genes than YZ-J, especially those associated with bacterial chemotaxis. In conclusion, the pan-genomic analysis provided new insights into the differential genetic content of the two strains.
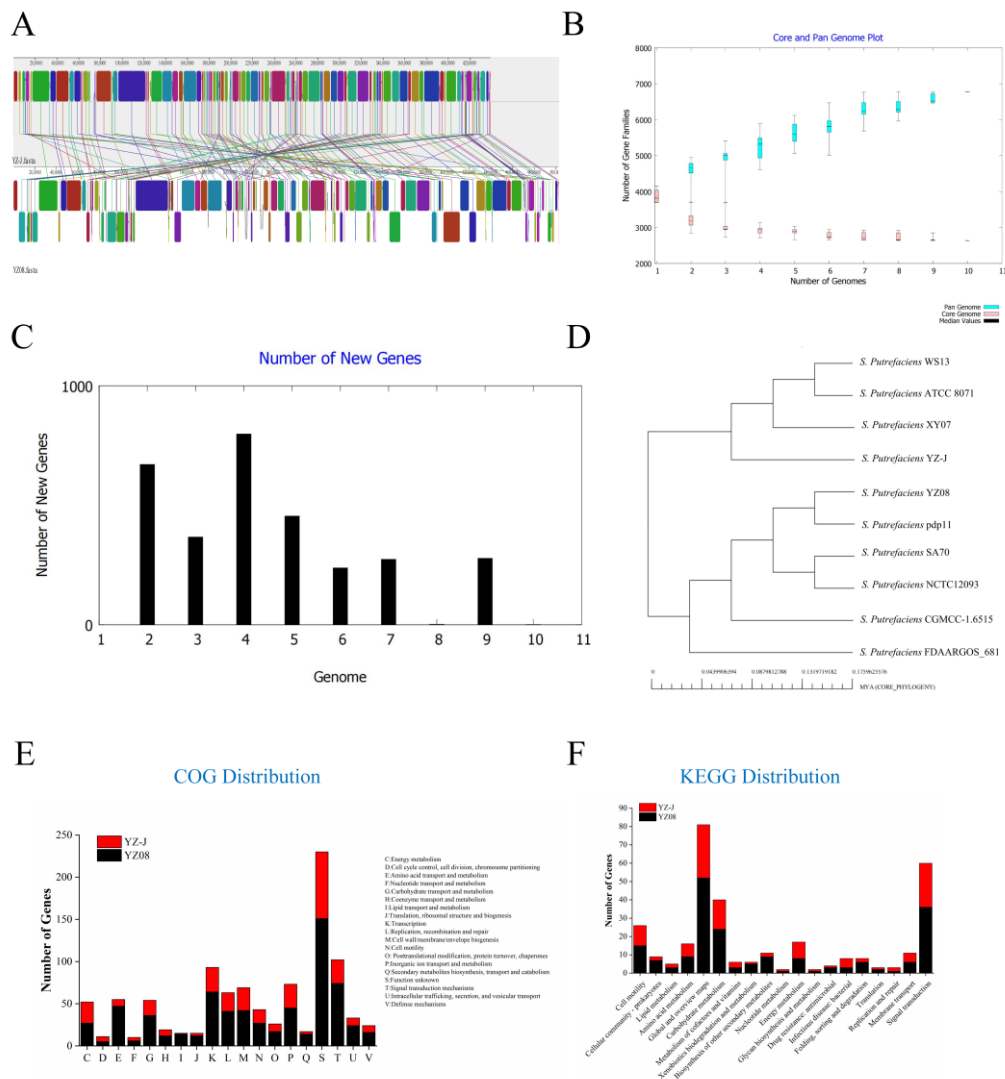


**Figure 3.** Genome synteny and pan-genome analysis of *S.putrefaciens*. (**A**) The mauve visualization of the whole genomes of *S. putrefaciens* YZ08 and YZ-J. The homologs distributed in these genomes are connected by lines; (**B**) pan-genome and core genome profile of different 10 *S. putrefaciens* strains; (**C**) prediction of increase in gene number when adding new genome; (**D**) phylogenetic tree based on pan genomes; (**E**) COG and (**F**) KEGG distribution of unique genes based on pan-genome of *S. putrefaciens* YZ08 and YZ-J.

### 3.3. Stress Adaptation

During food processing, microbes are subjected to a range of stresses, such as temperature, salt, pH, and nutrition stresses. The growth and biofilm formation of *S. putrefaciens* YZ08 and YZ-J under different stress conditions are shown in Figure 4. The growth of both

YZ08 and YZ-J in 5% NaCl and 20% LB was reduced compared with that in the control group (Figure 4A). The lag period for the growth of the two strains in the 4 °C groups was substantially longer than that of the control, but the maximum cell concentrations of the two strains were similar, which was consistent with the previous study [15]. The growth rate of YZ08 was higher than that of YZ-J in 5% NaCl; however, no significant differences were observed between the two strains for the other stress conditions. The Normalized biofilm formation rates of two strains in the 5% NaCl, 20% LB and 4 °C groups were higher than those in the control group, reaching significance in the 4 °C groups for both strains ($p < 0.05$) (Figure 4B). Low temperatures promote the expression of related genes to enhance the formation of biofilms [11]. Similarly, the higher normalized biofilm formation rates recorded under pH 6.0, 5% NaCl, and 20% LB stress relative to the control condition may be related to the formation of a greater amount of biofilm to protect the bacteria under stressful conditions [13]. In addition, the normalized biofilm decreased from 24 h to 144 h in the control, pH 6.0, NaCl 5%, and 4 °C groups, likely because the biofilm at this stage was in the dispersal period [34]. In all groups, the normalized biofilm formation of YZ08 was lower than that of YZ-J.
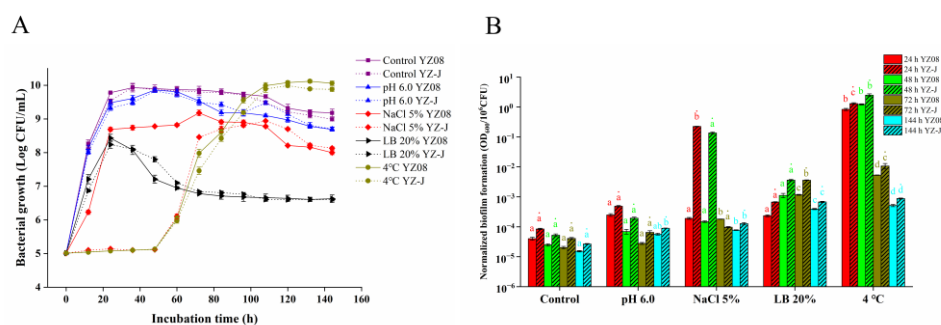


**Figure 4.** Growth curves (**A**) and biofilm formation (**B**) for *Shewanella putrefaciens* YZ08 and YZ-J under different stress conditions. The significance analysis of the same strain under different stress conditions at the same culture time was conducted; different lowercase letters indicate a significant difference ($p < 0.05$, the different styles of letters are used to distinguish the different groups).

A series of stress-related genes of *S. putrefaciens* YZ08 and YZ-J, including temperature, pH, NaCl, and nutrient stresses, is shown in Table 1. The cold shock genes *csp*A and *csp*D in *L. monocytogenes* are required to induce its growth at low temperatures [35,36] and may exert a similar function in *S. putrefaciens* YZ08 and YZ-J. Three *csp*A/*csp*D genes (K2227_07410, K2227_08825, K2227_12570, and K3G22_06460, K3G22_07485, K3G22_10845, respectively) were identified in the YZ08 and YZ-J genomes, which may explain the similar cold adaptability of the two strains. Furthermore, the genomes of both YZ08 and YZ-J contained eight genes encoding stress-related F0F1 ATP synthase, which is associated with the synthesis of ATP using ion translocation [37]. Interestingly, YZ08 contained six genes encoding sodium: proton antiporter and one encoding a transporter protein (K2227_13575) related to osmotic pressure, whereas YZ-J contained only four genes encoding sodium: proton transporters and none coding for the osmotic pressure-related transporter protein. This observation may partially explain the better growth of the YZ08 strain under 5% NaCl relative to that of strain YZ-J. The presence of genes encoding choline/glycine/proline betaine transporter and plasma membrane protein involved in salt tolerance indicated that *S. putrefaciens* maintains osmotic balance using a compatible solutes strategy when exposed to osmotic stress. RT-qPCR was used to study the expression of osmotic stress-related genes (encoding choline/glycine/proline betaine transporter and plasma membrane protein—K2227_07790 and K2227_01670, respectively, in YZ08 and K3G22_06825 and K3G22_01330, respectively, in YZ-J). As shown in Figure 5, the expression of the genes encoding choline/glycine/proline betaine transporter were significantly higher in strain YZ08 than in strain YZ-J ($p < 0.001$), which was consistent with YZ08 being better adapted to a high salt environment relative to YZ-J. However, the expression levels of the gene

encoding the plasma membrane protein did not show significant differences between in the two strains ($p > 0.05$). In addition, YZ08 and YZ-J shared similar genes encoding amino acid synthases.

**Table 1.** Stress-related genes of *S. putrefaciens* YZ08 and YZ-J.

| Stress | Gene | Encoded Protein | Locus Tag | |
|---|---|---|---|---|
| | | | **YZ08** | **YZ-J** |
| Temperature | *grp*E | Heat shock protein GrpE | K2227_15635 | K3G22_06000 |
| | *dna*K | Molecular chaperone DnaK | K2227_17110 | K3G22_14795 |
| | *dna*J | Molecular chaperone DnaJ | K2227_04710 K2227_09435 K2227_17105 | K3G22_07810 K3G22_14790 K3G22_15110 |
| | *hsl*R | Heat shock protein 15 | K2227_00795 | K3G22_18295 |
| | *hsl*J | Heat shock protein HslJ | K2227_17775 | K3G22_03895 |
| | *ibp*A | Heat shock protein IbpA | K2227_12130 | K3G22_10395 |
| | *htp*X | Heat shock protein HtpX | K2227_13200 | K3G22_11625 |
| | *csp*A | Cold shock protein | K2227_07410 K2227_08825 K2227_12570 | K3G22_06460 K3G22_07485 K3G22_10845 |
| | *groe*S | Co-chaperonin GroES (heat shock protein) | K2227_03200 | K3G22_02865 |
| | *groe*L | Molecular chaperone GroEL (heat shock protein) | K2227_03205 | K3G22_02870 |
| pH | *atp*C/*atp*D/*atp*G/ *atp*A/*atp*H/*atp*F/ *atp*E/*atp*B | F0F1 ATP synthase | K2227_21885 K2227_21890 K2227_21895 K2227_21900 K2227_21905 K2227_21910 K2227_21915 K2227_21920 | K3G22_19335 K3G22_19340 K3G22_19345 K3G22_19350 K3G22_19355 K3G22_19360 K3G22_19365 K3G22_19370 |
| | *pho*A/*pho*D | Alkaline phosphatase | K2227_03285 K2227_03290 K2227_04030 | K3G22_15755 |
| NaCl | *nha*D/*nha*C/*Yui*F | Sodium: proton antiporter | K2227_06070 K2227_06375 K2227_10490 K2227_10855 K2227_17710 K2227_20195 | K3G22_03965 K3G22_05205 K3G22_09220 K3G22_17770 |
| | *env*Z | Osmolarity sensor histidine kinase EnvZ | K2227_21175 | K3G22_00555 |
| | *omp*R | Transcriptional regulatory protein OmpR | K2227_21170 | K3G22_00560 |
| | | Choline/glycine/proline betaine transport protein | K2227_07790 | K3G22_06825 |
| | | Plasma membrane protein involved in salt tolerance | K2227_01670 | K3G22_01330 |

**Table 1.** *Cont.*

| Stress | Gene | Encoded Protein | Locus Tag | |
|---|---|---|---|---|
| | | | **YZ08** | **YZ-J** |
| Nutrient | *pur*A | Adenylosuccinate synthetase | K2227_03495 K2227_16420 | K3G22_03065 K3G22_14060 |
| | *thi*C | Hydroxymethyl-pyrimidine synthase | K2227_11880 | K3G22_09485 |
| | *pab*B | Aminodeoxychorismate synthase component 1 | K2227_10065 | K3G22_08745 |
| | *pan*C | Pantothenate synthetase | K2227_04225 | K3G22_15605 |
| | *arg*G | Argininosuccinate synthase | K2227_20520 | K3G22_18080 |
| | *cys*M | Cysteine synthase B | K2227_05310 | K3G22_04610 |
| | *cys*K | Cysteine synthase A | K2227_13820 | K3G22_11825 |
| | *met*H | Methionine synthase | K2227_04845 K2227_16165 | K3G22_13880 K3G22_14750 |
| | *gln*A | Glutamine synthetase | K2227_01730 K2227_05875 | K3G22_01380 K3G22_05075 |
| | *thr*C | Threonine synthase | K2227_16000 | K3G22_13695 |
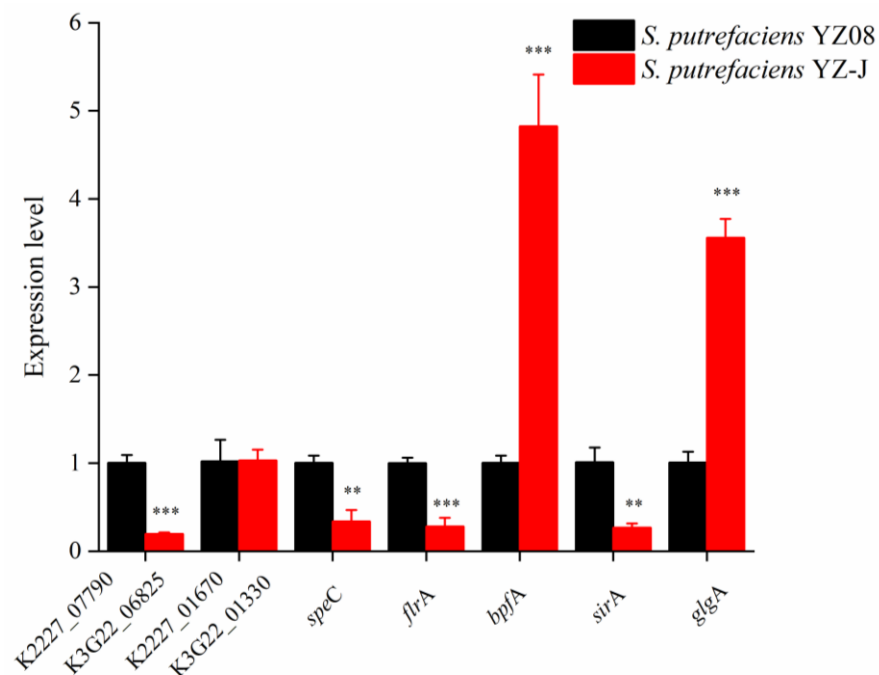


**Figure 5.** Comparison of the expression levels of biofilm formation-related and spoilage-related genes associated with salt stress between *Shewanella putrefaciens* strains YZ-J and YZ08. Gene expression levels in *S. putrefaciens* YZ-J are expressed as values relative to the control group (*S. putrefaciens* YZ08). ** $p < 0.01$, *** $p < 0.001$.

*3.4. Motility*

Cell surface characteristics (chemotactic systems) and motility are critical during biofilm formation [38]. *S. putrefaciens* motility (swimming and swarming) is shown in Figure 6. The swimming motility of both YZ08 and YZ-J increased in a time-dependent manner at the optimal growth temperature (30 °C), but swimming behavior began late at low temperatures (4 °C), especially for strain YZ-J (Figure 6A). The swimming ability of YZ08 strain at the two temperatures was stronger than that of strain YZ-J, which may

have been due to the stronger movement ability of the polar flagella of YZ08, as previously described for *Vibrio parahaemolyticus* RIMD2210633. [39]. The swimming abilities of the two *S. putrefaciens* strains were stronger than those of *S. baltica* SB02 and *S. baltica* OS155 [24,40]. Differences in genes encoding chemotaxis proteins and the regulation of some differential key genes such as *flg*M, encoding an important regulatory factor for flagella gene expression; *zom*B, encoding a flagellar motor control protein; and genes encoding PilZ domain proteins, may explain the different swimming phenotypes of the two strains [41,42]. In contrast to their strong swimming abilities, the swarming abilities of *S. putrefaciens* YZ08 and YZ-J were weak, and also showed a time dependence (Figure 6B). At 30 °C, the difference in swarming ability between the two strains was not significant, while at 4 °C the swarming ability of YZ08 was slightly stronger than that of YZ-J. The absence of lateral flagella may explain the weaker swarming ability of *Shewanella* spp. relative to *Vibrio* spp. [39,43]. No genes encoding lateral flagella were found in either strain in this study, which would account for their weak swarming ability.
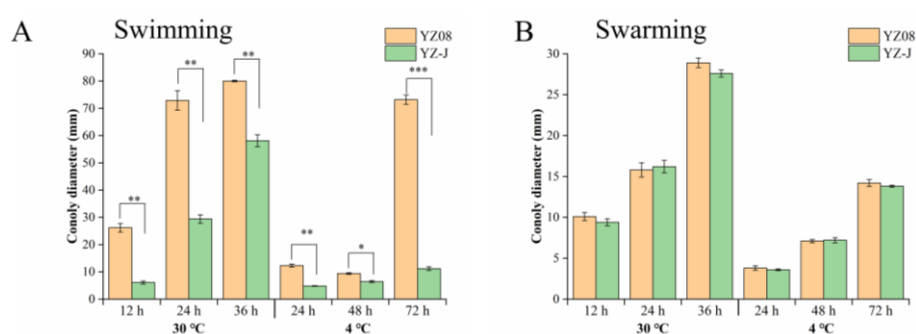


**Figure 6.** Swimming (**A**) and swarming (**B**) motility of *S. putrefaciens* YZ08 and YZ-J in LB performed at 15 and 30 °C. no mark $p > 0.05$, * $p < 0.05$, ** $p < 0.01$, *** $p < 0.001$.

Table 2 lists most of the motility-associated genes in YZ08 and YZ-J. No differences were found between the two strains for the three gene clusters encoding polar flagellins (A-I, A-II, and A-III). A-I contains structural genes coding for sodium-driven motor rings, loops and hook proteins, and assembly and chaperone proteins, as previously described in *Vibrio* [44]. The A-II gene cluster contains genes encoding regulatory proteins, filaments, basal bodies, switch proteins, and export proteins. The deletion of these genes can lead to the loss of motility in bacteria, as previously described in *Pseudomonas fluorescens* F113 [45]. The third cluster (A-III) contains chemotaxis genes, export genes, and regulatory genes that express late flagellar genes encoding filament proteins, motor proteins, and other flagellar-associated secretory proteins, as previously described [46]. In addition to genes encoding flagellins, those coding for chemotaxis proteins are also critical for bacterial motility [47]. The YZ08 strain contained up to 19 genes encoding chemotaxis proteins compared with only 13 for YZ-J (Table 2), which may explain the markedly greater swimming ability of YZ08 relative to that of YZ-J.

**Table 2.** Genes associated with motility, biogenic amine metabolism, trimethylamine metabolism, sulfur metabolism, biofilm formation, and exopolysaccharide formation in *S. putrefaciens* YZ08 and YZ-J.

| | Gene | Encoded Protein | Locus Tag | |
| --- | --- | --- | --- | --- |
| | | | YZ08 | YZ-J |
| Motility | A-I | Basal body rod, rings, hook, and regulation protein | K2227_15200- K2227_15275 | K3G22_12995- K3G22_13070 |
| | A-II | Filament, basal body, switch, and export proteins | K2227_15080- K2227_15195 | K3G22_12875- K3G22_12990 |

**Table 2.** *Cont.*

| Gene | Encoded Protein | Locus Tag | |
|---|---|---|---|
| | | **YZ08** | **YZ-J** |
| A-III | Regulatory, export, chemotaxis, and motor proteins | K2227_15020-<br>K2227_15075<br>K2227_15610<br>K2227_15615<br>K2227_03500<br>K2227_03505 | K3G22_12815-<br>K3G22_12870<br>K3G22_17150<br>K3G22_17155<br>K3G22_06020<br>K3G22_06025 |
| *che*X | Chemotaxis proteins | K2227_03560<br>K2227_11490<br>K2227_11495<br>K2227_11500<br>K2227_11510<br>K2227_11515<br>K2227_11520<br>K2227_13440<br>K2227_14420<br>K2227_15020<br>K2227_15025<br>K2227_15050<br>K2227_15055<br>K2227_15255<br>K2227_15260<br>K2227_15040<br>K2227_15045<br>K2227_16425K2227_19145 | K3G22_03130<br>K3G22_11550<br>K3G22_12430<br>K3G22_12815<br>K3G22_12820<br>K3G22_12835<br>K3G22_12840<br>K3G22_12845<br>K3G22_12850<br>K3G22_13050<br>K3G22_13055<br>K3G22_14065<br>K3G22_16555 |
| *zom*B | Flagellar motor control protein ZomB | K2227_12675 | K3G22_10945 |
| *pilZ* | Pilz domain-containing protein | K2227_08445<br>K2227_12485<br>K2227_16555<br>K2227_16565 | K3G22_07390<br>K3G22_10760<br>K3G22_14160<br>K3G22_14170 |
| *mcp* | Methyl-accepting chemotaxis protein | K2227_01520<br>K2227_01560<br>K2227_04495<br>K2227_05180<br>K2227_05395<br>K2227_05730<br>K2227_05985<br>K2227_07050<br>K2227_09095<br>K2227_09850<br>K2227_10100<br>K2227_11990<br>K2227_13265<br>K2227_14075<br>K2227_14105<br>K2227_15425<br>K2227_15910<br>K2227_15945<br>K2227_17160<br>K2227_17180<br>K2227_17310<br>K2227_17445<br>K2227_17510<br>K2227_17895<br>K2227_18115<br>K2227_18355<br>K2227_18980<br>K2227_20645<br>K2227_20825<br>K2227_21180 | K3G22_01230<br>K3G22_01265<br>K3G22_01935<br>K3G22_02480<br>K3G22_02665<br>K3G22_02720<br>K3G22_03550<br>K3G22_04190<br>K3G22_04340<br>K3G22_04510<br>K3G22_04680<br>K3G22_05125<br>K3G22_05590<br>K3G22_06750<br>K3G22_06810<br>K3G22_08945<br>K3G22_09970<br>K3G22_10280<br>K3G22_10305<br>K3G22_12080<br>K3G22_13645<br>K3G22_14785<br>K3G22_15015<br>K3G22_15195<br>K3G22_15940<br>K3G22_16410<br>K3G22_18525 |

**Table 2.** *Cont*.

| | Gene | Encoded Protein | Locus Tag | |
|---|---|---|---|---|
| | | | YZ08 | YZ-J |
| Biogenic amines metabolism | *puu*P | Putrescine importer PuuP | K2227_02810 | K3G22_02305 |
| | *puu*B | Gamma-glutamylputrescine oxidoreductase | K2227_05900 | K3G22_05100 |
| | *pot*F | Putrescine transport system substrate-binding protein | K2227_05880 | K3G22_05080 |
| | *pot*G | Putrescine transport ATP-binding protein | K2227_05885 | K3G22_05085 |
| | *pot*H | Spermidine/putrescine ABC transporter permease | K2227_05890 | K3G22_05090 |
| | *pot*I | Putrescine transport system permease protein | K2227_05895 | K3G22_05095 |
| | *pot*E | Putrescine-ornithine antiporter | K2227_20335 | K3G22_17905 |
| | *spe*C | Ornithine/lysine decarboxylase | K2227_20330 | K3G22_17900 |
| | *spe*A | Biosynthetic arginine decarboxylase | K2227_09155 | K3G22_07940 |
| | *lys*E | Lysine transporter | K2227_05120 K2227_10525 | K3G22_02835 K3G22_06765 |
| Trimethylamine metabolism | *tor*E | Trimethylamine N-oxide reductase system protein TorE | K2227_16520 | — |
| | *tor*C | Pentaheme c-type cytochrome TorC | K2227_16525 | — |
| | *tor*A | Trimethylamine-N-oxide reductase TorA | K2227_16530 | — |
| | *tor*D | Molecular chaperone TorD | K2227_16535 | — |
| | *tor*S | TMAO reductase system sensor histidine kinase/response regulator TorS | K2227_16540 | — |
| | *tor*T | TMAO reductase system periplasmic protein TorT | K2227_16545 | — |
| | *tor*R | Two-component system response regulator TorR | K2227_16550 | — |
| | *pfl*D | Formate C-acetyltransferase | K2227_13855 | K3G22_11865 |
| | *pfl*A | Pyruvate formate lyase 1-activating protein | K2227_13860 | K3G22_11870 |
| Sulfur metabolism | *cys*E | Serine O-acetyltransferase | K2227_12190 | K3G22_10455 |
| | *cys*Z | Sulfate transporter | K2227_13805 | K3G22_11810 |
| | *cys*K | Cysteine synthase A | K2227_13820 | K3G22_11825 |
| | *cys*Q | $3'(2'),5'$-bisphosphate nucleotidase | K2227_00930 K2227_07435 | K3G22_18190 K3G22_06480 |
| | *cys*J | Sulfite reductase [NADPH] flavoprotein alpha-component | K2227_04610 | K3G22_15255 |
| | *cys*I | Sulfite reductase (NADPH) hemoprotein, beta-component | K2227_04615 | K3G22_15250 |
| | *cys*H | Phosphoadenylyl-sulfate reductase | K2227_04620 | K3G22_15245 |
| | *cys*D | Sulfate adenylyltransferase subunit 2 | K2227_04650 | K3G22_15150 |
| | *cys*N | Sulfate adenylyltransferase subunit 1 | K2227_04655 | K3G22_15145 |
| | *cys*C | adenylyl-sulfate kinase | K2227_04665 | K3G22_15135 |
| | *cys*A | Sulfate transport system ATP-binding protein | K2227_05290 | K3G22_04590 |
| | *cys*W | Sulfate transport system permease protein | K2227_05295 | K3G22_04595 |
| | *cys*U | sulfate/thiosulfate ABC transporter permease | K2227_05300 | K3G22_04600 |
| | *cys*P | Thiosulfate ABC transporter substrate-binding | K2227_05305 | K3G22_04605 |

**Table 2.** *Cont.*

| | Gene | Encoded Protein | Locus Tag | |
|---|---|---|---|---|
| | | | YZ08 | YZ-J |
| | *cys*M | Cysteine synthase B | K2227_05310 | K3G22_04610 |
| | *sir*A | Dissimilatory sulfite reductase SirA | K2227_19420 | K3G22_16750 |
| | *phs*A | Thiosulfate reductase | K2227_02935 | K3G22_02440 |
| | *met*B | Cystathionine gamma-synthase | K2227_02960 | K3G22_02465 |
| | *sse*A | 3-mercaptopyruvate sulfurtransferase | K2227_05850 | K3G22_05050 |
| | *met*A | Homoserine O-succinyltransferase | K2227_07535 | K3G22_06595 |
| | *ttr*R | Tetrathionate response regulatory protein | K2227_18710 | K3G22_02690 |
| | *ttr*S | Tetrathionate sensor histidine kinase | K2227_18715 | K3G22_02685 |
| | *ttr*B | Tetrathionate reductase subunit B | K2227_18720 | K3G22_02680 |
| | *ttr*C | Tetrathionate reductase subunit C | K2227_18725 | K3G22_02675 |
| | *ttr*A | Tetrathionate reductase subunit A | K2227_18730 | K3G22_02670 |
| | *glp*E | Thiosulfate sulfurtransferase | K2227_21760 | K3G22_00255 |
| Bilofilm formation | *gsp*X | Type II secretion system protein | K2227_00800<br>K2227_00805<br>K2227_00810<br>K2227_00815<br>K2227_00820<br>K2227_00825<br>K2227_00830<br>K2227_00835<br>K2227_00840<br>K2227_00845<br>K2227_00850<br>K2227_00855<br>K2227_06060<br>K2227_06065 | K3G22_02165<br>K3G22_05200<br>K3G22_18235<br>K3G22_18240<br>K3G22_18245<br>K3G22_18250<br>K3G22_18255<br>K3G22_18260<br>K3G22_18265<br>K3G22_18270<br>K3G22_18275<br>K3G22_18280<br>K3G22_18285<br>K3G22_18290 |
| | *omp*R | Two-component system, OmpR family, phosphate regulon response regulator OmpR | K2227_21170 | K3G22_00560 |
| | *env*Z | Two-component system, OmpR family, osmolarity sensor histidine kinase EnvZ | K2227_21175 | K3G22_00555 |
| | *cya*A | class I adenylate cyclase | K2227_19915 | K3G22_17425 |
| | *csg*B | Minor curlin subunit | K2227_04215 | K3G22_15615 |
| | *cpd*A | 3′,5′-cyclic-AMP phosphodiesterase | K2227_03910 | K3G22_03185 |
| | *crp/vfr* | cAMP-activated global transcriptional regulator CRP | K2227_18785 | K3G22_02620 |
| | *trp*E | anthranilate synthase component 1 | K2227_13995 | K3G22_11985 |
| | *trp*G | aminodeoxychorismate/anthranilate synthase component II | K2227_14000 | K3G22_11990 |
| | *msh*E | MSHA biogenesis protein MshE | K2227_02690 | K3G22_02185 |
| | *msh*B | MSHA pilin protein MshB | K2227_02705 | K3G22_02200 |
| | *msh*A | MSHA pilin protein MshA | K2227_02710 | K3G22_02205 |
| | *msh*C | MSHA pilin protein MshC | K2227_02715 | K3G22_02210 |
| | *msh*D | MSHA pilin protein MshD | K2227_02720 | K3G22_02215 |
| | *flr*C | Two-component system, response regulator FlrC | K2227_15155 | K3G22_12950 |
| | *flr*B | Two-component system, sensor histidine kinase FlrB | K2227_15160 | K3G22_12955 |
| | *flr*A/*fle*Q | Sigma-54 dependent transcriptional regulator | K2227_15165 | K3G22_12960 |
| | *fli*A | RNA polymerase sigma factor FliA | K2227_15060 | K3G22_12855 |

**Table 2.** *Cont.*

| Gene | Encoded Protein | Locus Tag | |
|---|---|---|---|
| | | YZ08 | YZ-J |
| *flg*M | Flagellar biosynthesis anti-sigma factor FlgM | K2227_15270 | K3G22_13065 |
| *lux*S | S-ribosylhomocysteine lyase | K2227_17240 | K3G22_04260 |
| *csr*A | carbon storage regulator CsrA | K2227_16070 | K3G22_13785 |
| *gac*S/*bar*A | Two-component sensor histidine kinase | K2227_16195 | K3G22_13910 |
| *gac*A/*uvr*Y | Two-component response regulator transcription factor | K2227_13250 | K3G22_07880 |
| *rpo*S | RNA polymerase sigma factor RpoS | K2227_16100 | K3G22_13815 |
| *rpo*N | RNA polymerase factor sigma-54 | K2227_03400 | K3G22_02925 |
| *rpo*D | RNA polymerase sigma factor RpoD | K2227_06000 | K3G22_05135 |
| *aph*B | LysR family transcriptional regulator, AphB | K2227_17170 | K3G22_04330 |
| *hfq* | RNA chaperone Hfq | K2227_18885 | K3G22_16320 |
| *fis* | DNA-binding transcriptional regulator Fis | K2227_19855 | K3G22_17135 |
| *crr* | PTS glucose transporter subunit IIA | K2227_12010 | K3G22_10300 |
| *hap* | M4 family metallopeptidase | K2227_02450 | - |
| *cdg*C | c-di-GMP phosphodiesterase | K2227_03335 | - |
| *dks*A | RNA polymerase-binding protein DksA | K2227_04250 | K3G22_15580 |
| *gcv*A | Transcriptional regulator GcvA | K2227_15595 | K3G22_06040 |
| *gcv*R | glycine cleavage system transcriptional repressor | K2227_13180 | K3G22_08205 |
| *arc*A | Two-component system response regulator ArcA | K2227_18630 | K3G22_02750 |
| *bpf*A | Biofilm-promoting protein BpfA | K2227_19940 | K3G22_17455 |
| | Type I secretion system permease/ATPase | K2227_19945 | K3G22_17460 |
| | HlyD family type I secretion periplasmic adaptor subunit | K2227_19950 | K3G22_17465 |
| | TolC family outer membrane protein | K2227_19955 | K3G22_17470 |
| | OmpA family protein | K2227_19960 | K3G22_17475 |
| | Transglutaminase-like cysteine peptidase | K2227_19965 | K3G22_17480 |
| | EAL domain-containing protein | K2227_19970 | K3G22_17485 |
| Exopolysaccharide formation — *glg*A | Glycogen synthase | K2227_15730 | K3G22_05905 |
| *glg*C | Glucose-1-phosphate adenylyltransferase | K2227_15735 | K3G22_05900 |
| *glg*P | glycogen/starch/alpha-glucan phosphorylase | K2227_15740 | K3G22_05895 |
| *glg*B | 1,4-alpha-glucan branching protein GlgB | K2227_15750 | K3G22_05885 |
| *pgm* | Phosphoglucomutase | K2227_10900 | K3G22_09265 |

### 3.5. Spoilage-Related Metabolic Pathways

*S. putrefaciens* usually generates spoilage metabolites such as total volatile base nitrogen (TVB-N), TMA, and biogenic amines (BAs) in seafood, leading to a decline in its quality [7]. The spoilage potential of *S. putrefaciens* is associated with sulfur metabolism, BAs metabolism, TMA metabolism, and protease secretion [2].

### 3.5.1. Biogenic Amines (BAs) Metabolism

Putrescine, cadaverine, and histamine are common BAs found in spoiled tuna [48]. However, as *S. putrefaciens* is mainly associated with the production of putrescine and

cadaverine, and generates only limited amounts of histamine [49]. We focused on investigating the putrescine and cadaverine production activities in the two *S. putrefaciens* strains. The amounts of putrescine and cadaverine produced by YZ08 and YZ-J at 30 and 4 °C using ornithine, arginine, and lysine as substrates are shown in Figure 7A,B. The findings indicated that YZ08 produced greater amounts of putrescine and cadaverine than YZ-J at both the optimum growth temperature and low temperature. We also found that both *S. putrefaciens* strains produced more putrescine than cadaverine, which may be because putrescine can be produced using different substrates (ornithine and arginine) and through different pathways, whereas cadaverine is produced through only one pathway (lysine decarboxylation) [22].
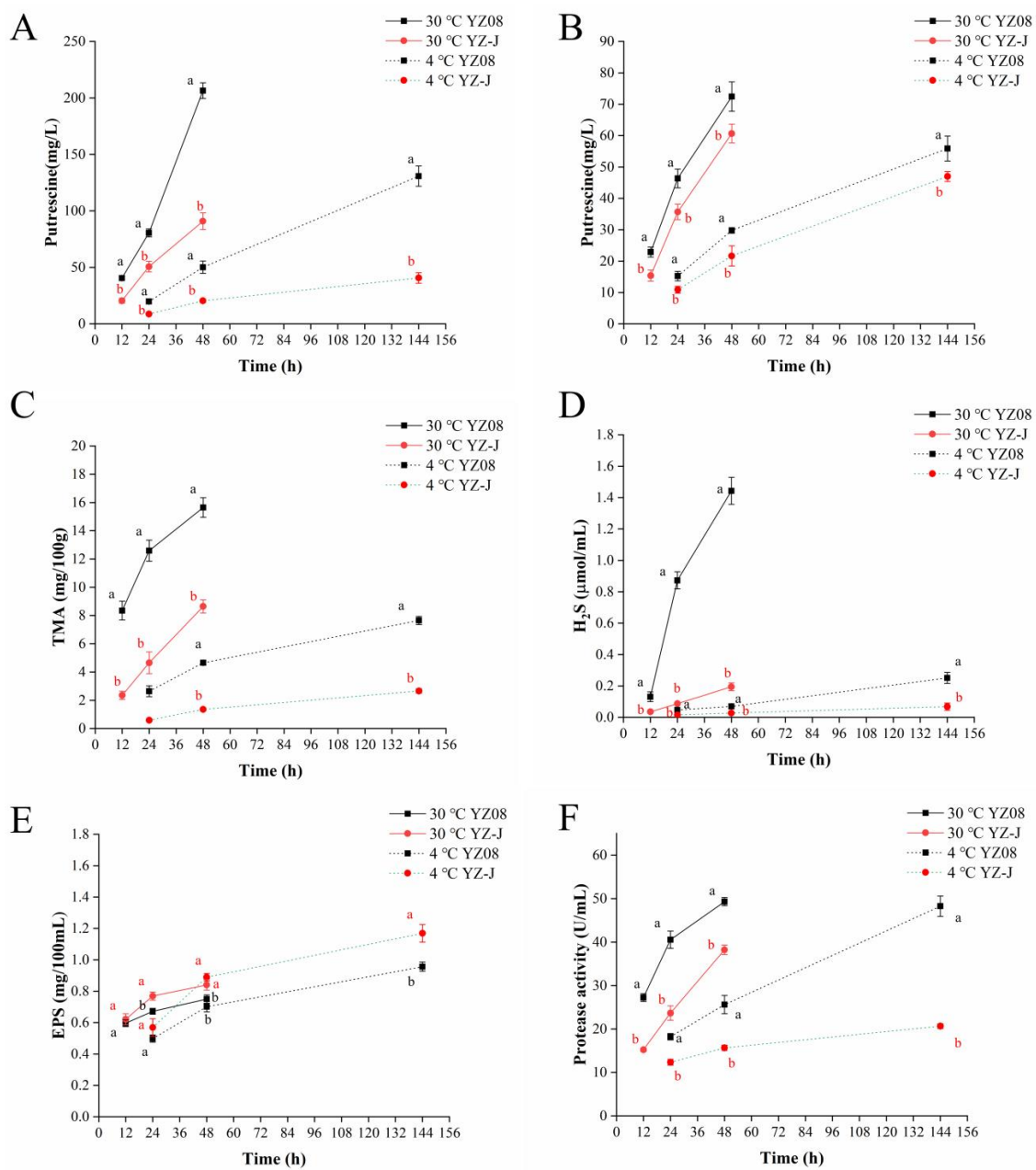


**Figure 7.** Changes in the putrescine (**A**), cadaverine (**B**), TMA (**C**), H$_2$S (**D**), exopolysaccharide (**E**) and protease activity (**F**) produced by *S. putrefaciens* YZ08 and YZ-J during storage at 4 and 30 °C. The significance analysis for different strains at the same culture time and temperature was performed. Different lowercase letters indicate significant differences ($p < 0.05$).

The genomic analysis identified several BA-related genes in the two tested strains (Table 2). Several *pot* genes involved in putrescine metabolism were identified in *S. putrefaciens*, including genes encoding substrate-binding proteins of the putrescine transport system, a putrescine transport ATP-binding protein, spermidine/putrescine ABC transporter permease, putrescine transport system permease protein, and a putrescine-ornithine antiporter. In addition, genes encoding putrescine importer PuuP and gamma-glutamylputrescine oxidoreductase were also found in the genomes of both strains. In *S. putrefaciens* CN32, ornithine decarboxylase is a key enzyme capable of producing putrescine from L-ornithine [2]. Similarly, arginine is converted to cadaverine by ornithine/arginine decarboxylase. The presence of ornithine/arginine decarboxylase corroborated the production of putrescine and cadaverine by the two strains. Although no difference was found in putrescine-related genes, the levels of putrescine and cadaverine production in YZ08 and YZ-J were different, indicating that some regulatory factors could induce the expression of these genes. The results of qRT-PCR supported this hypothesis, indicating that the expression of *spe*C in *S.putrefaciens* YZ08 was significantly higher than that in YZ-J ($p < 0.01$, Figure 5).

### 3.5.2. TMA Metabolism

As mentioned earlier, most *Shewanella* spp. can reduce TMAO to TMA and produce a fishy odor. Figure 7C shows the amount of TMA produced by YZ08 and YZ-J in LB medium containing TMAO at 4 and 30 °C. At both temperatures, the amount of TMA produced by YZ08 was significantly higher than that of YZ-J ($p < 0.05$). As shown in Table 2, genes encoding trimethylamine N-oxide reductase system protein TorE (K2227_16520), pentaheme c-type cytochrome TorC (K2227_16525), trimethylamine-N-oxide reductase TorA (K2227_16530), molecular chaperone TorD (K2227_16535), histidine kinase TorS (K2227_16540), periplasmic protein TorT (K2227_16545), and response regulator TorR (K2227_16550) were found in YZ08, but not found in YZ-J. The same TMA metabolism related genes were identified in other strains (*S. baltica* OS155 and 128) [13,50]. Although no trimethylamine metabolism-related genes were found in YZ-J, this strain also produced small amounts of TMA, suggestive of the existence of other trimethylamine metabolism pathways. It has been reported that gut microbiota can metabolize compounds containing trimethylamine groups to produce TMA from the precursors of TMA containing choline, phosphatidylcholine, and glycerophosphatidylcholine. The key genes involved in this process are *cut*C, encoding a choline TMA-lyase and gene *cut*D, encoding a choline TMA-lyase activase [51]. In the present study, *pfl*A/D genes, homologs of *cut*C/D were found in *S. putrefaciens* YZ08 and YZ-J. *cut*D and *pfl*D are related to pyruvate formate lyase activating enzyme, and *cut*C and *pfl*A are homologous to pyruvate formate lyase. Therefore, a small amount of TMA produced in *S. putrefaciens* YZ-J may be related to the presence of *pfl*A/D.

### 3.5.3. Sulfur Metabolism

$H_2S$ gas has a characteristic off-odor and is associated with the presence of *Shewanella* spp. during the spoilage of seafood [2]. In this study, we explored the $H_2S$ content produced by *S. putrefaciens* YZ08 and YZ-J (Figure 7D). At 30 °C, YZ08 produced a significant amount of $H_2S$ in the fish juice. However, at the low temperature (4 °C), both strains generated low amounts of $H_2S$ at the end of storage (144 h). In general, YZ08 metabolized more $H_2S$ than YZ-J. The genes associated with sulfur metabolism in YZ08 and YZ-J are listed in Table 2. Sulfate is converted to adenosine 5′-phosphosulfate (APS) by sulfate adenylyltransferase (encoded by the *cys*N gene). APS is then converted to 3′-phosphonoadenosine-5′-phosphate sulfate (PAPS) by the action of adenylyl-sulfate kinase (encoded by *cys*C), which is then further reduced to sulfite by phosphonoadenosine phosphate reductase (encoded by *cys*H). Finally, sulfite is reduced to sulfide by dissimilatory sulfite reductase (encoded by *sir*A). Moreover, the *ttr*SRBC encoding tetrathionate response regulatory protein, tetrathionate sensor histidine kinase, tetrathionate reductase subunit B and cysteine synthase C was also identified in the genomes of both *S. putrefaciens* strains, suggesting that tetrathionate may be reduced and eventually form sulfide through the activity of these enzymes, consistent with

the findings of Leustek et al. [52]. That the two strains contained the same sulfur metabolism genes, suggests that they produce different amounts of $H_2S$. This could be explained by differences in the transcription levels given that the level of *Sir*A was significantly greater in YZ08 than in YZ-J ($p < 0.01$) (Figure 5). Highly similar genes related to sulfur metabolism were found in *S. baltica* 128 and *S. putrefaciens* YZ07.

### 3.5.4. Biofilm and Exopolysaccharide Formation

Biofilms have a strong adhesive ability, and they envelop bacteria, thereby enhancing their resistance to adverse environments [53]. On the surface of food processing equipment, some spoilage microorganisms, and pathogenic microorganisms form biofilms. These biofilms are resistant to disinfectants and are difficult to clear, thus affecting food quality and safety. In this study, both strains of *S. putrefaciens* produced biofilms; however, YZ-J produced a significantly greater amount of biofilm than YZ08 at both temperatures (4 and 30 °C) tested (Figure 4B). The genes associated with biofilm formation in YZ08 and YZ-J are listed in Table 2. The key factors regulating biofilm formation of *Escherichia coli* and *Pseudomonas aeruginosa* include c-di-GMP regulatory system, the cAMP/Vfr pathway, and the two-component regulatory system GacS-GacA and EnvZ-ompR [54,55]. The presence of the above genes in the genomes of both YZ08 and YZ-J suggested that there may be multiple pathways regulating biofilm formation in two strains. The mechanisms involved in biofilm regulation in *Shewanella* spp. are poorly understood but are thought to be primarily related to the c-di-GMP pathway. c-di-GMP is synthesized by diguanylate cyclase (DGC) from two molecules of GTP and is decomposed into two molecules of GTP through the activity of phosphodiesterase (PDE) [56]. Several genes encoding DGC and PDE were found in the genomes of both YZ08 and YZ-J (data not shown). However, the *cdg*C gene encoding c-di-GMP PDE was only found in YZ08 (Table 2). Both *Shewanella putrefaciens* CN32 and *Shewanella oneidensis* MR-1 possess a conserved operon containing seven genes [57,58], and this operon also exists in YZ08 and YZ-J. The operon encodes an adhesion protein BpfA; a type I secretion system responsible for the secretion of BpfA into the extracellular compartment (a type I secretion system permease/ATPase, a HlyD family type I secretion periplasmic adaptor subunit, a TolC family outer membrane protein and an OmpA family protein); the protease that regulates BpfA activity (transglutaminase-like cysteine peptidase) and the c-di-GMP receptor protein (EAL domain-containing protein). The secretion of the adhesion protein BpfA in *Shewanella* promotes bacterial adhesion to solid surface, and the bacteria lacking this protein cannot form biofilms [59].

When the intracellular c-di-GMP content is low, the transcription factor FlrA can promote flagellar operon transcription and repress *bpf*A operon transcription by directly binding to the promoter region of *bpf*A, and ultimately biofilm formation is inhibited. When the intracellular c-di-GMP level is high, c-di-GMP binds to and forms a complex with the transcription factor FlrA, thereby relieving the transcriptional activation of flagellar-related genes and the transcriptional repression of the *bpf*A operon. Eventually, the bacterium undergoes irreversible initiation of adsorption and biofilm formation [59]. c-di-GMP also activates the transcriptional regulator RpoS, thereby upregulating the expression of biofilm-associated genes [24]. The amount of biofilm of YZ-J was greater than that of YZ08, which may be due to the higher content of c-di-GMP and the weak motility in YZ-J. Although there are many regulatory mechanisms for biofilm formation, the mechanism for biofilm formation in *Shewanella* spp. mainly involves regulation of the secretion of the adhesion protein BpfA by the FlrA factor. Accordingly, we explored the differences in the expression levels of *flr*A and *bpf*A between the two strains. The RT-qPCR results showed that the expression of *flr*A, encoding an inhibitor of biofilm formation, was significantly higher, and that of *bpf*A significantly lower, in the YZ08 strain than in the YZ-J strain (both $p < 0.01$) (Figure 5), which was in line with the higher amount of biofilm formation in strain YZ-J relative to that in strain YZ08.

Exopolysaccharide is an important component of bacterial biofilms, and bacteria can promote microcolony formation and biofilm maturation by regulating exopolysaccharide

synthesis [60]. Similar to the pattern of biofilm formation, the levels of exopolysaccharide produced by YZ-J were significantly higher than those generated by YZ08 at the end of storage (Figure 7E). The genes responsible for exopolysaccharide synthesis in both strains are listed in Table 2. No genes responsible for the biosynthesis of the polysaccharides alginate, Psl, Pel, or that of any other exopolysaccharide, were identified in the genome of either strain. Only glycogen synthesis genes were found. Glucose 6-phosphate is converted to glucose 1-phosphate by the phosphoglucomutase (encoded by *pgm*), following which glucose 1-phosphate is converted to ADP-glucose through the activity of glucose-1-phosphate adenyltransferase (encoded by *glg*C). ADP-glucose is subsequently used to extend the $\alpha$-1,4-glucosidic chain through glycogen synthase (encoded by *glg*A), after which branching enzyme (encoded by *glg*B) catalyzes the formation of $\alpha$-1,6-linked branch chains, yielding glycogen. Glycogen is broken down into glucose by glycogen phosphatase (encoded by *glg*P) [61]. In our study, RT-qPCR results (Figure 5) showed that the expression of *glg*A in *S. putrefaciens* YZ-J was significantly higher than in *S. putrefaciens* YZ08 ($p < 0.001$), which could explain the higher production of exopolysaccharides in the former.

### 3.5.5. Protease and Lipase

Proteases and lipases secreted by spoilage bacteria hydrolyze, respectively, protein and fat in seafood, thus reducing its quality [62]. The protease and lipase activity of *S. putrefaciens* YZ08 and YZ-J is shown in Figures 7F and 8. The protease activity of YZ08 was found to be significantly greater than that of YZ-J ($p < 0.05$). The results also showed that YZ08 had substantially larger protease hydrolysis halos than YZ-J, and that no protease hydrolysis halo was seen for YZ-J at 4 °C (Figure 8A,B). However, the lipolytic activity of YZ08 was slightly lower than that of YZ-J, although the difference was not significant (Figure 8E).
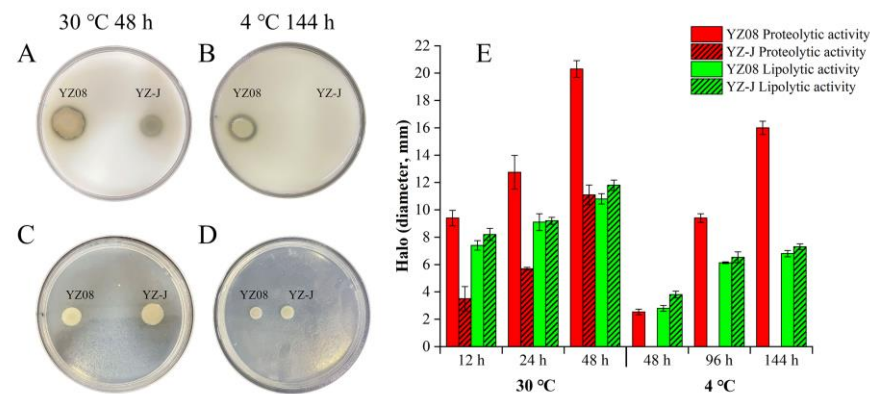


**Figure 8.** Halos associated with proteolytic (measured on agar plates containing 5% skimmed milk) (**A**,**B**) and lipase (measured on triglyceride agar) (**C**,**D**) activity of *Shewanella putrefaciens* YZ08 and YZ-J following incubation at 4 and 30 °C for 48 and 144 h. Bars in the graphs represent the mean diameter of clear proteolytic and lipolytic halos at 30 °C for 12, 24, and 48 h and 4 °C for 48, 96, and 144 h (**E**).

Genes encoding protease and lipase from in the YZ08 and YZ-J genomes are listed in Table 3. There were differences in the genes encoding proteases that contain signal peptides between YZ08 and YZ-J. Signal peptides in enzymes are necessary for enzyme secretion [63], and extracellular protease secreted by bacteria generally contains a signal peptide. Here, we found that YZ08 contained two genes encoding M48 family metallopro-teases (K2227_09265 and K2227_17060) and one encoding an M4 family metallopeptidase (Hap) while YZ-J had only one gene encoding M48 family metalloprotease (K3G22_08175). YZ08, but not YZ-J, also contained a gene encoding an alkaline serine protease. Moreover, we found that YZ-J lacked protease activity at 4 °C (no halo was produced on skimmed milk-containing), which may be related to absence of any gene encoding an alkaline serine

protease in this strain, which usually still exhibited activity over a large temperature range (0–50 °C) [64]. YZ08 and YZ-J shared the same lipase encoding gene, likely explaining why the two strains showed similar lipolytic activity. Genes encoding alkaline serine proteases have also been found in *S. baltica* 128 and *S. putrefaciens* XY07, while the *hap* gene was found in only *S. baltica* 128. Genes encoding lipases were found in both *S. baltica* 128 and *S. putrefaciens* XY07.

**Table 3.** Genes encoding proteases and lipases of *S. putrefaciens* YZ08 and YZ-J.

| | Gene | Encoded Protein | Locus Tag | | Signal Peptide |
|---|---|---|---|---|---|
| | | | YZ08 | YZ-J | |
| Protease | *ctp*A | Carboxyl-terminal protease | K2227_00255 | K3G22_19255 | No |
| | *hap* | M4 family metallopeptidase | K2227_02450 | - | Yes |
| | *hsl*U | ATP-dependent protease ATPase subunit HslU | K2227_02475 | K3G22_02010 | No |
| | *hsl*V | ATP-dependent protease subunit HslV | K2227_02480 | K3G22_02015 | No |
| | *tld*D | Metalloprotease TldD | K2227_02775 | K3G22_02275 | No |
| | *pmb*A | Metalloprotease PmbA | K2227_02825 | K3G22_02340 | No |
| | *deg*S | Outer membrane-stress sensor serine endopeptidase DegS | K2227_03465 | K3G22_03035 | No |
| | *spr*T | SprT family zinc-dependent metalloprotease | K2227_04050 | K3G22_15735 | No |
| | *glu*P | Rhomboid family intramembrane serine protease | K2227_04770 | K3G22_00250 | No |
| | *res*P | Sigma E protease regulator RseP | K2227_07350 | K3G22_06405 | No |
| | *clp*P | ATP-dependent Clp endopeptidase proteolytic subunit ClpP | K2227_08100 | K3G22_07070 | No |
| | *clp*X | ATP-dependent protease ATP-binding subunit ClpX | K2227_08105 | K3G22_07075 | No |
| | *lon* | Endopeptidase La | K2227_08110 | K3G22_07080 | No |
| | *bep*A | M48 family metalloprotease | K2227_09265 K2227_17060 | K3G22_08175 | Yes |
| | *clp*A | ATP-dependent Clp protease ATP-binding subunit ClpA | K2227_12560 | K3G22_10835 | No |
| | *htp*X | Protease HtpX | K2227_13200 | K3G22_11625 | No |
| | *soh*B | Protease SohB | K2227_13950 | K3G22_11940 | No |
| | *fst*H | ATP-dependent zinc metalloprotease FtsH | K2227_16705 | K3G22_14305 | No |
| | | Alkaline serine protease | K2227_16455 | — | Yes |
| | *glg*G | Rhomboid family intramembrane serine protease glgG | K2227_21765 | K3G22_04125 | No |
| | | Transglutaminase-like cysteine peptidase | K2227_19965 | K3G22_17475 | Yes |
| Lipase | *pld*A | Phospholipase A | K2227_04640 | K3G22_15160 | Yes |
| | | Lipase | K2227_13955 | K3G22_11945 | Yes |
| | | Patatin-like phospholipase family protein | K2227_14815 K2227_19695 | K3G22_12635 K3G22_16980 | Yes |
| | *pho*D | Alkaline phosphatase D family protein | K2227_18295 | K3G22_15860 | Yes |
| | *rss*A | Patatin-like phospholipase RssA | K2227_08360 | K3G22_07315 | No |

## 4. Conclusions

In this study, we analyzed the phenotypic traits (environmental stress, BAs metabolism, TMA metabolism, sulfur metabolism, biofilm formation, exopolysaccharide production, motility, extracellular protease, and lipase activity) and the whole genomes of *S. putrefaciens* YZ08 and YZ-J to identify the genomic determinants of their spoilage-related phenotypes. Although YZ08 and YZ-J were found to be genetically similar, the phenotypic analysis indicated that significant differences in responses to NaCl stress, motility, and

spoilage-related metabolism existed between the two strains. Strain YZ08 displayed better growth than YZ-J under NaCl stress, which may be relevant to the presence of more genes encoding sodium:proton antiporter and the high expression of a gene encoding a choline/glycine/proline betaine transporter protein in the YZ08 strain. YZ08 also was found to have greater swimming motility than YZ-J, which was consistent with the greater number of *che*X genes found in the former strain. The strong swimming motility and the low transcript levels of the *bpf*A gene, possibly due to low c-di-GMP content, likely resulted in a low biofilm-forming capacity for YZ08. The lower production of exopolysaccharides in YZ08 relative to YZ-J may be related to the low expression of *glg*A, which encodes glycogen synthase. The lack of the TMA metabolism-related operon *tor*ECADSTR may explain the lower TMA generation in YZ-J. The presence of genes encoding extracellular proteases (alkaline serine protease and M4 family metallopeptidase) may be important factors causing low extracellular protease activity of YZ-J. Overall, some differences in the genetic factors of two strains were consistent with the phenotypic differences. This study contributes to the understanding of the molecular mechanisms underlying the spread, motility, and spoilage activity of two strains of *S. putrefaciens*.

**Supplementary Materials:** The following supporting information can be downloaded at: https://www.mdpi.com/article/10.3390/foods11091261/s1, Table S1: quantitative real-time PCR primers used in this study; Table S2: unique genes of *S. putrefaciens* YZ08 by pan-genome analysis between *S. putrefaciens* YZ08 and YZ-J.; Table S3: unique genes of *S. putrefaciens* YZ-J by pan-genome analysis between *S. putrefaciens* YZ08 and YZ-J.

**Author Contributions:** Z.Y.: conceptualization, methodology, software, investigation, writing. J.X.: validation, formal analysis, writing—review and editing, examination, funding acquisition. All authors have read and agreed to the published version of the manuscript.

**Institutional Review Board Statement:** Not applicable.

**Informed Consent Statement:** Not applicable.

**Data Availability Statement:** Data is contained within the article and Supplementary Materials.

**Conflicts of Interest:** The authors declare no conflict of interest.

## References

1. Gram, L.; Huss, H.H. Microbiological spoilage of fish and fish products. *Int. J. Food Microbiol.* **1996**, *33*, 121–137. [CrossRef]
2. Remenant, B.; Jaffrès, E.; Dousset, X.; Pilet, M.-F.; Zagorec, M. Bacterial spoilers of food: Behavior, fitness and functional properties. *Food Microbiol.* **2015**, *45*, 45–53. [CrossRef]
3. Anagnostopoulos, D.A.; Parlapani, F.F.; Boziaris, I.S. The evolution of knowledge on seafood spoilage microbiota from the 20th to the 21st century: Have we finished or just begun? *Trends Food Sci. Technol.* **2022**, *120*, 236–247. [CrossRef]
4. Boziaris, I.S.; Parlapani, F.F. Specific Spoilage Organisms (SSOs) in Fish. In *The Microbiological Quality of Food*; Elsevier: Amsterdam, The Netherlands, 2017; pp. 61–98.
5. Odeyemi, O.A.; Burke, C.M.; Bolch, C.C.J.; Stanley, R. Seafood spoilage microbiota and associated volatile organic compounds at different storage temperatures and packaging conditions. *Int. J. Food Microbiol.* **2018**, *280*, 87–99. [CrossRef]
6. Lee, B.H.; Wu, S.C.; Shen, T.L.; Hsu, Y.Y.; Chen, C.H.; Hsu, W.H. The applications of *Lactobacillus plantarum*-derived extracellular vesicles as a novel natural antibacterial agent for improving quality and safety in tuna fish. *Food Chem.* **2021**, *340*, 128104. [CrossRef]
7. Qian, Y.-F.; Xie, J.; Yang, S.-P.; Wu, W.-H.; Xiong, Q.; Gao, Z.-L. In vivo study of spoilage bacteria on polyphenoloxidase activity and melanosis of modified atmosphere packaged Pacific white shrimp. *Food Chem.* **2014**, *155*, 126–131. [CrossRef]

8. Vogel, B.F.; Venkateswaran, K.; Satomi, M.; Gram, L. Identification of *Shewanella baltica* as the Most Important H2S-Producing Species during Iced Storage of Danish Marine Fish. *Appl. Environ. Microbiol.* **2005**, *71*, 6689–6697. [CrossRef]
9. Fu, L.; Wang, C.; Liu, N.; Ma, A.; Wang, Y. Quorum sensing system-regulated genes affect the spoilage potential of *Shewanella baltica*. *Food Res. Int.* **2018**, *107*, 1–9. [CrossRef]
10. Yi, Z.; Xie, J. Assessment of spoilage potential and amino acids deamination & decarboxylation activities of *Shewanella putrefaciens* in bigeye tuna (*Thunnus obesus*). *LWT* **2022**, *156*, 113016. [CrossRef]
11. Yan, J.; Xie, J. Comparative Proteome Analysis of *Shewanella putrefaciens* WS13 Mature Biofilm Under Cold Stress. *Front. Microbiol.* **2020**, *11*, 1225. [CrossRef]
12. Li, Y.; Jia, S.; Hong, H.; Zhang, L.; Zhuang, S.; Sun, X.; Liu, X.; Luo, Y. Assessment of bacterial contributions to the biochemical changes of chill-stored blunt snout bream (*Megalobrama amblycephala*) fillets: Protein degradation and volatile organic compounds accumulation. *Food Microbiol.* **2020**, *91*, 103495. [CrossRef]
13. Li, J.; Yu, H.; Yang, X.; Dong, R.; Liu, Z.; Zeng, M. Complete genome sequence provides insights into the quorum sensing-related spoilage potential of *Shewanella baltica* 128 isolated from spoiled shrimp. *Genomics* **2020**, *112*, 736–748. [CrossRef]
14. Chen, L.; Yang, S.; Qian, Y.; Xie, J. Sequencing and Analysis of the *Shewanella putrefaciens* WS13 Genome. *J. Biobased Mater. Bioenergy* **2019**, *13*, 182–187. [CrossRef]
15. Yang, S.-P.; Xie, J.; Cheng, Y.; Zhang, Z.; Zhao, Y.; Qian, Y.-F. Response of *Shewanella putrefaciens* to low temperature regulated by membrane fluidity and fatty acid metabolism. *LWT* **2020**, *117*, 108638. [CrossRef]
16. Yi, Z.; Xie, J. Prediction in the Dynamics and Spoilage of *Shewanella putrefaciens* in Bigeye Tuna (*Thunnus obesus*) by Gas Sensors Stored at Different Refrigeration Temperatures. *Foods* **2021**, *10*, 2132. [CrossRef]
17. Cai, L.; Zheng, S.-W.; Shen, Y.-J.; Zheng, G.-D.; Liu, H.-T.; Wu, Z.-Y. Complete genome sequence provides insights into the biodrying-related microbial function of *Bacillus thermoamylovorans* isolated from sewage sludge biodrying material. *Bioresour. Technol.* **2018**, *260*, 141–149. [CrossRef]
18. Tatusov, R.L.; Koonin, E.V.; Lipman, D.J. A Genomic Perspective on Protein Families. *Science* **1997**, *278*, 631–637. [CrossRef]
19. Darling, A.C.E.; Mau, B.; Blattner, F.R.; Perna, N.T. Mauve: Multiple Alignment of Conserved Genomic Sequence With Rearrangements. *Genome Res.* **2004**, *14*, 1394–1403. [CrossRef]
20. Chaudhari, N.M.; Gupta, V.K.; Dutta, C. BPGA—An ultra-fast pan-genome analysis pipeline. *Sci. Rep.* **2016**, *6*, 24373. [CrossRef]
21. Dyer, W.J. Amines in Fish Muscle: I. Colorimetric Determination of Trimethylamine as the Picrate Salt. *J. Fish. Res. Board Can.* **1945**, *6d*, 351–358. [CrossRef]
22. Zhuang, S.; Liu, X.; Li, Y.; Zhang, L.; Hong, H.; Liu, J.; Luo, Y. Biochemical changes and amino acid deamination & decarboxylation activities of spoilage microbiota in chill-stored grass carp (*Ctenopharyngodon idella*) fillets. *Food Chem.* **2021**, *336*, 127683. [CrossRef] [PubMed]
23. Hong, H.; Luo, Y.; Zhou, Z.; Bao, Y.; Lu, H.; Shen, H. Effects of different freezing treatments on the biogenic amine and quality changes of bighead carp (*Aristichthys nobilis*) heads during ice storage. *Food Chem.* **2013**, *138*, 1476–1482. [CrossRef] [PubMed]
24. Feng, L.; Bi, W.; Chen, S.; Zhu, J.; Liu, X. Regulatory function of sigma factors RpoS/RpoN in adaptation and spoilage potential of *Shewanella baltica*. *Food Microbiol.* **2021**, *97*, 103755. [CrossRef]
25. DuBois, M.; Gilles, K.A.; Hamilton, J.K.; Rebers, P.A.; Smith, F. Colorimetric Method for Determination of Sugars and Related Substances. *Anal. Chem.* **1956**, *28*, 350–356. [CrossRef]
26. Anbu, P. Characterization of solvent stable extracellular protease from *Bacillus koreensis* (BK-P21A). *Int. J. Biol. Macromol.* **2013**, *56*, 162–168. [CrossRef] [PubMed]
27. Lowry, O.H.; Rosebrough, N.J.; Farr, A.L.; Randall, R.J. Protein measurement with the Folin phenol reagent. *J. Biol. Chem.* **1951**, *193*, 265–275. [CrossRef]
28. Livak, K.J.; Schmittgen, T.D. Analysis of Relative Gene Expression Data Using Real-Time Quantitative PCR and the $2^{-\Delta\Delta CT}$ Method. *Methods* **2001**, *25*, 402–408. [CrossRef] [PubMed]
29. Lange, H.; Kaut, A.; Kispal, G.; Lill, R. A mitochondrial ferredoxin is essential for biogenesis of cellular iron-sulfur proteins. *Proc. Natl. Acad. Sci. USA* **2000**, *97*, 1050–1055. [CrossRef]
30. Pajor, A.M.; Sun, N.N. Nonsteroidal Anti-Inflammatory Drugs and Other Anthranilic Acids Inhibit the $Na^+$/Dicarboxylate Symporter from *Staphylococcus aureus*. *Biochemistry* **2013**, *52*, 2924–2932. [CrossRef]
31. Gang, H.; Xiao, C.; Xiao, Y.; Yan, W.; Bai, R.; Ding, R.; Yang, Z.; Zhao, F. Proteomic analysis of the reduction and resistance mechanisms of *Shewanella oneidensis* MR-1 under long-term hexavalent chromium stress. *Environ. Int.* **2019**, *127*, 94–102. [CrossRef]
32. Paul, R.; Abel, S.; Wassmann, P.; Beck, A.; Heerklotz, H.; Jenal, U. Activation of the Diguanylate Cyclase PleD by Phosphorylation-mediated Dimerization. *J. Biol. Chem.* **2007**, *282*, 29170–29177. [CrossRef]
33. Higgins, C. ABC Transporters: From Mircoorganisms to Man. *Annu. Rev. Cell Dev. Biol.* **1992**, *8*, 67–113. [CrossRef]
34. Mukherjee, M.; Zaiden, N.; Teng, A.; Hu, Y.; Cao, B. Shewanella biofilm development and engineering for environmental and bioenergy applications. *Curr. Opin. Chem. Biol.* **2020**, *59*, 84–92. [CrossRef]
35. Kragh, M.L.; Muchaamba, F.; Tasara, T.; Truelstrup Hansen, L. Cold-shock proteins affect desiccation tolerance, biofilm formation and motility in Listeria monocytogenes. *Int. J. Food Microbiol.* **2020**, *329*, 108662. [CrossRef]
36. Chan, Y.C.; Raengpradub, S.; Boor, K.J.; Wiedmann, M. Microarray-Based Characterization of the Listeria monocytogenes Cold Regulon in Log- and Stationary-Phase Cells. *Appl. Environ. Microbiol.* **2007**, *73*, 6484–6498. [CrossRef]

37.  Zhang, W.; Guo, H.; Cao, C.; Li, L.; Kwok, L.-Y.; Zhang, H.; Sun, Z. Adaptation of *Lactobacillus casei* Zhang to Gentamycin Involves an Alkaline Shock Protein. *Front. Microbiol.* **2017**, *8*, 2316. [CrossRef]

38.  Quintieri, L.; Caputo, L.; De Angelis, M.; Fanelli, F. Genomic Analysis of Three Cheese-Borne *Pseudomonas lactis* with Biofilm and Spoilage-Associated Behavior. *Microorganisms* **2020**, *8*, 1208. [CrossRef]

39.  Cao, J.; Liu, H.; Wang, Y.; He, X.; Jiang, H.; Yao, J.; Xia, F.; Zhao, Y.; Chen, X. Antimicrobial and antivirulence efficacies of citral against foodborne pathogen *Vibrio parahaemolyticus* RIMD2210633. *Food Control* **2021**, *120*, 107507. [CrossRef]

40.  Wang, F.; Wang, Y.; Cen, C.; Fu, L.; Wang, Y. A tandem GGDEF-EAL domain protein-regulated c-di-GMP signal contributes to spoilage-related activities of *Shewanella baltica* OS155. *Appl. Microbiol. Biotechnol.* **2020**, *104*, 2205–2216. [CrossRef]

41.  Brenzinger, S.; Pecina, A.; Mrusek, D.; Mann, P.; Völse, K.; Wimmi, S.; Ruppert, U.; Becker, A.; Ringgaard, S.; Bange, G.; et al. ZomB is essential for flagellar motor reversals in *Shewanella putrefaciens* and *Vibrio parahaemolyticus*. *Mol. Microbiol.* **2018**, *109*, 694–709. [CrossRef]

42.  Pecina, A.; Schwan, M.; Blagotinsek, V.; Rick, T.; Klüber, P.; Leonhard, T.; Bange, G.; Thormann, K.M. The Stand-Alone PilZ-Domain Protein MotL Specifically Regulates the Activity of the Secondary Lateral Flagellar System in *Shewanella putrefaciens*. *Front. Microbiol.* **2021**, *12*, 1160. [CrossRef]

43.  Wu, L.; Wang, J.; Tang, P.; Chen, H.; Gao, H. Genetic and Molecular Characterization of Flagellar Assembly in *Shewanella oneidensis*. *PLoS ONE* **2011**, *6*, e21479. [CrossRef]

44.  Terashima, H.; Koike, M.; Kojima, S.; Homma, M. The Flagellar Basal Body-Associated Protein FlgT Is Essential for a Novel Ring Structure in the Sodium-Driven Vibrio Motor. *J. Bacteriol.* **2010**, *192*, 5609–5615. [CrossRef] [PubMed]

45.  Capdevila, S.; Martínez-Granero, F.M.; Sánchez-Contreras, M.; Rivilla, R.; Martín, M. Analysis of *Pseudomonas fluorescens* F113 genes implicated in flagellar filament synthesis and their role in competitive root colonization. *Microbiology* **2004**, *150*, 3889–3897. [CrossRef] [PubMed]

46.  Chevance, F.F.V.; Hughes, K.T. Coordinating assembly of a bacterial macromolecular machine. *Nat. Rev. Microbiol.* **2008**, *6*, 455–465. [CrossRef]

47.  Charon, N.W.; Cockburn, A.; Li, C.; Liu, J.; Miller, K.A.; Miller, M.R.; Motaleb, M.A.; Wolgemuth, C.W. The Unique Paradigm of Spirochete Motility and Chemotaxis. *Annu. Rev. Microbiol.* **2012**, *66*, 349–370. [CrossRef]

48.  Jaguey-Hernández, Y.; Aguilar-Arteaga, K.; Ojeda-Ramirez, D.; Añorve-Morga, J.; González-Olivares, L.G.; Castañeda-Ovando, A. Biogenic amines levels in food processing: Efforts for their control in foodstuffs. *Food Res. Int.* **2021**, *144*, 110341. [CrossRef]

49.  López-Caballero, M.; Sánchez-Fernández, J.; Moral, A. Growth and metabolic activity of *Shewanella putrefaciens* maintained under different $CO_2$ and $O_2$ concentrations. *Int. J. Food Microbiol.* **2001**, *64*, 277–287. [CrossRef]

50.  Wang, Y.; Wang, F.; Wang, C.; Li, X.; Fu, L. Positive regulation of spoilage potential and biofilm formation in *Shewanella baltica* OS155 via quorum sensing system composed of DKP and orphan LuxRs. *Front. Microbiol.* **2019**, *10*, 135. [CrossRef]

51.  Craciun, S.; Balskus, E.P. Microbial conversion of choline to trimethylamine requires a glycyl radical enzyme. *Proc. Natl. Acad. Sci. USA* **2012**, *109*, 21307–21312. [CrossRef]

52.  Leustek, T.; Martin, M.N.; Bick, J.-A.; Davies, J.P. Pathways and regulation of sulfur metabolism revealed through molecular and genetic studies. *Annu. Rev. Plant Physiol. Plant Mol. Biol.* **2000**, *51*, 141–165. [CrossRef] [PubMed]

53.  Flemming, H.-C.; Wingender, J.; Szewzyk, U.; Steinberg, P.; Rice, S.A.; Kjelleberg, S. Biofilms: An emergent form of bacterial life. *Nat. Rev. Microbiol.* **2016**, *14*, 563–575. [CrossRef]

54.  Gosset, G.; Zhang, Z.; Nayyar, S.; Cuevas, W.A.; Saier, M.H. Transcriptome Analysis of Crp-Dependent Catabolite Control of Gene Expression in *Escherichia coli*. *J. Bacteriol.* **2004**, *186*, 3516–3524. [CrossRef] [PubMed]

55.  Rasamiravaka, T.; Labtani, Q.; Duez, P.; El Jaziri, M. The Formation of Biofilms by Pseudomonas aeruginosa: A Review of the Natural and Synthetic Compounds Interfering with Control Mechanisms. *BioMed Res. Int.* **2015**, *2015*, 759348. [CrossRef] [PubMed]

56.  Sondermann, H.; Shikuma, N.J.; Yildiz, F.H. You've come a long way: C-di-GMP signaling. *Curr. Opin. Microbiol.* **2012**, *15*, 140–146. [CrossRef]

57.  Zhou, G.; Yuan, J.; Gao, H. Regulation of biofilm formation by BpfA, BpfD, and BpfG in *Shewanella oneidensis*. *Front. Microbiol.* **2015**, *6*, 790. [CrossRef]

58.  Wu, C.; Cheng, Y.-Y.; Yin, H.; Song, X.-N.; Li, W.-W.; Zhou, X.-X.; Zhao, L.-P.; Tian, L.-J.; Han, J.-C.; Yu, H.-Q. Oxygen promotes biofilm formation of *Shewanella putrefaciens* CN32 through a diguanylate cyclase and an adhesin. *Sci. Rep.* **2013**, *3*, 1945. [CrossRef]

59.  Cheng, Y.-Y.; Wu, C.; Wu, J.-Y.; Jia, H.-L.; Wang, M.-Y.; Wang, H.-Y.; Zou, S.-M.; Sun, R.-R.; Jia, R.; Xiao, Y.-Z. FlrA Represses Transcription of the Biofilm-Associated bpfA Operon in *Shewanella putrefaciens*. *Appl. Environ. Microbiol.* **2017**, *83*, e02410–e02416. [CrossRef]

60.  Jenal, U.; Reinders, A.; Lori, C. Cyclic di-GMP: Second messenger extraordinaire. *Nat. Rev. Microbiol.* **2017**, *15*, 271–284. [CrossRef]

61.  Ballicora, M.A.; Iglesias, A.A.; Preiss, J. ADP-Glucose Pyrophosphorylase, a Regulatory Enzyme for Bacterial Glycogen Synthesis. *Microbiol. Mol. Biol. Rev.* **2003**, *67*, 213–225. [CrossRef]

62.  Chen, S.-C.; Adams, A.; Richards, R.H. Extracellular products from *Mycobacterium* spp. in fish. *J. Fish Dis.* **1997**, *20*, 19–25. [CrossRef]

63.  Liu, Y.; Shi, C.; Li, D.; Chen, X.; Li, J.; Zhang, Y.; Yuan, H.; Li, Y.; Lu, F. Engineering a highly efficient expression system to produce BcaPRO protease in *Bacillus subtilis* by an optimized promoter and signal peptide. *Int. J. Biol. Macromol.* **2019**, *138*, 903–911. [CrossRef] [PubMed]
64.  Damare, S.; Raghukumar, C.; Muraleedharan, U.D.; Raghukumar, S. Deep-sea fungi as a source of alkaline and cold-tolerant proteases. *Enzym. Microb. Technol.* **2006**, *39*, 172–181. [CrossRef]